2001

Impedance Feedback Control for Scanning Electrochemical Microscopy

David O. Wipf
Mississippi State University, dow1@msstate.edu

Mario A. Apuche-Avlles

Impedance Feedback Control for Scanning Electrochemical Microscopy

Mario A. Alpuche-Aviles and David O. Wipf*, Department of Chemistry,

Mississippi State University, Mississippi State MS 39762

Published Version: Impedance Feedback Control for Scanning Electrochemical Microscopy Mario A. Alpuche-Aviles and David O. Wipf, *Analytical Chemistry* **2001** *73*, 4873-4881. https://dx.doi.org/10.1021/ac010581q

Abstract

A new constant-distance imaging method based on the relationship between tip impedance and tip-substrate separation has been developed for the scanning electrochemical microscope (SECM). The tip impedance is monitored by application of a high frequency ac voltage bias between the tip and auxiliary electrode. The high frequency ac current is easily separated from the dc level faradaic electrochemistry with a simple RC filter, which allows impedance measurements during feedback or generation/collection experiments. By employing a piezo-based feedback controller we are able to maintain the impedance at a constant value and, thus, maintain a constant tip-substrate separation. Application of the method to feedback and generation/collection experiments with tip electrodes as small as 2 μm is presented.

Submitted to Analytical Chemistry, May 17, 2001, Revised July 17, 2001

*wipf@ra.msstate.edu

Introduction

The scanning electrochemical microscope (SECM) is a scanning probe method that employs an electrochemically active tip. In most experiments the tip is an amperometric ultramicroelectrode (UME) of micron or submicron dimension. [1-3] In the feedback mode, an intentionally added mediator is electrolyzed at the scanning tip. At close tip-substrate separation, the electrochemical current is a function of the separation and the nature of the substrate.[4] At a conducting substrate, the mediator can be restored to its original oxidation state by electron transfer between the mediator and substrate. The mediator is thus cycled between oxidized and reduced forms in the tip-substrate gap. The recycling is most efficient at close separations and, thus, the tip current increases as tip-substrate distance decreases. In the *positive feedback mode* the mediator-substrate electron transfer is diffusion controlled and the tip current depends on the tip-substrate separation and the tip geometry. However, the tip current is also very sensitive to the rate of electron transfer between mediator and substrate and, for non diffusion-controlled electron transfer, the tip current is also a function of the local electron-transfer rate at the substrate (reaction-rate imaging). In *negative feedback* an insulating surface prevents electron transfer and thus the tip current decreases as the tip approaches the substrate. The non-conducting sample blocks diffusion of the mediator at the probe. Because tip-current response is different when a tip approaches a conducting, insulating, or reactive surface, the tip current cannot be used to unambiguously determine the tip-substrate separation in feedback mode. Variations of the current can be due either to a change in conductivity, electron-transfer, or topography of the area of study. Additional information is required to distinguish these possibilities.

In amperometric generation/collection (GC) mode the tip is used to map the concentration of electroactive species in solution. Often the goal is to correlate the presence of species near a surface with some surface chemical reaction (e.g. corrosion [5-7] or biological process [8-12]). A major limitation to this technique is that the tip-current is insensitive to the separation between tip and substrate and thus positioning the tip at the surface requires additional information, such as video microscopy.

Most SECM experiments employ *constant-height* imaging, where the tip is scanned in reference plane above the sample. Since no allowance is made for sample tilt or large relief changes, much care in preparing flat, untilted samples is necessary. In addition, high-relief samples essentially cannot be imaged with constant-height imaging. For feedback and GC mode the best image resolution occurs when the probe is separated by a tip diameter or less. Thus, as tips become smaller, constant height imaging becomes increasingly unattractive. *Constant-distance* imaging, where the tip follows the sample topography during scanning, is preferred. However, except under restricted circumstances, the SECM tip current signal is unable to supply the information required to maintain a constant tip-substrate separation. It is then desirable to develop a method that can continuously provide tip-sample separation information but does not interfere with the normal SECM tip current.

A number of methods have been proposed to provide constant-distance imaging. Tip-position modulation, TPM, uses a small amplitude (10 nm) vertical oscillation of the probe that is used to determinate the nature of the substrate.[13, 14] In feedback mode, the tip oscillation produces a modulated current that changes phase by 180° as the tip moves from an insulating to a conducting region of the substrate. A discriminator, employing phase-sensitive detection, determines the conductivity of the

substrate and sets the servo-controller set point and loop gain as necessary for conductive or insulating surfaces. Since the conductivity of the surface is determined independently, the dc tip current is used to maintain a constant tip-substrate separation. Note, however, that the current modulation gives no information about the surface conductivity in the GC mode and, thus, TPM mode is not useful for GC imaging.

Another approach is to borrow the shear-force technique first employed in the near-field scanning optical microscope (NSOM) where an optical fiber is scanned very close to a surface (~20 nm).[15, 16] Shear force was first applied to SECM by Shumann and co-workers[17] who used a piezo-electric actuator to laterally oscillate a specially built tip electrode. As the tip approaches the surface, the oscillation is damped due to the hydrodynamic forces between the tip and the solution. Smyrl and co-workers modified an NSOM tip by coating it with metal and insulating paint to form an SECM tip, which was then attached to one of the arms of a quartz tuning fork.[18-20] The presence of the surface is noted by a shift in the resonance frequency of the tuning fork/probe assembly. Constant-distance imaging is possible by using a servo controller to maintain tuning fork output and, hence, a constant distance. Shear-force imaging works with both feedback and GC modes but requires special electrode design.[21] In addition, the tip resonance is effectively damped by solution, thus special samples cell employing thin layers of solution are required for good results.[22]

Macpherson and Unwin have developed an SECM tip that can be used in an atomic force microscope (AFM).[23] The AFM tip is prepared from a 50 μm Pt wire that is bent into a cantilever, etched to produce a conical tip, and insulated with electrophoretic paint. This AFM-SECM tip is mounted on a commercial microscope, and can collect contact-mode AFM images while simultaneously acquiring high-resolution

electrochemical information. The AFM-SECM tip allows collection of high-resolution topography as well as feedback or GC SECM data. However, it requires an AFM controller and fabrication of special tips.

We present in this paper a constant-distance control method that uses standard SECM tips and can operate with feedback and GC imaging. It is based on the change of tip-electrode impedance at the tip as a function of the distance between the scanning probe and sample. A similar method of position control is used in the scanning ion conductance microscopy (SICM). [24-26] In this technique, a micropipette filled with a conducting solution is scanned over an isolating substrate. The dc current that flows between the micropipette and a counter electrode can be used as a feedback control signal to scan the surface because the impedance increases when the tip gets closer to the surface. A similar method has been used to position ion selective SECM tips for GC mode imaging.[27-29] Impedance detection was used because potentiometric tips do not have well defined approach curves, which makes the determination of the tip-sample separation difficult. By detecting the impedance of the solution in the tip-sample gap, the position of potentiometric electrodes could be calibrated either before, or during the potential measurements. In this work we demonstrate that impedance measurements and electrochemical experiments can be made simultaneously at the same tip. By multiplexing the impedance measurement and the electrochemical signal the tip is used to provide independent topographic and electrochemical information. We achieve this by applying a high frequency bias voltage to the tip, causing a small ac current to flow through the solution in the probe-sample gap. The amount of current depends on the impedance of the solution in the gap and this provides a control signal for a feedback controller.

Experimental Section

Reagents $Ru(NH_3)_6Cl_3$ was used as received from Strem Chemicals (Newburyport, MA) All other reagents were ACS grade and used as received. $Ru(NH_3)_6Cl_3$ solutions were prepared in pH=3.2 phosphate-citrate (McIlvaine) buffer made to 0.5 M ionic strength with KCl and $K_3Fe(CN)_6$ solutions were prepared in 0.5 M KCl adjusted to pH=2. All solutions were prepared using distilled-deionized water (Nanopure, Barnstead)

Electrodes Imaging tips were 2.0- and 10-μm diameter Pt disks, glass insulated and built as described previously by sealing Pt wire (Goodfellow Metals, Ltd., Cambridge, UK) into soft glass.[30, 31] The substrate was constructed from a 10 μm diameter Pt disk sealed in glass and embedded in epoxy resin. The reference electrode was either Ag/AgCl in 3M KCl or an SCE. A Pt wire served as an auxiliary electrode. The scanning and the substrate electrodes were polished with 0.05 μm alumina before each experiment.

Instrumentation The basic SECM instrumentation has been described elsewhere,[6] briefly, a micropositioner based on "inchworm" piezoelectric motors (Burleigh Instruments, Fishers, New York) allows three-dimensional tip movement. A bipotentiostat (EI 400 Ensman instrumentation, Bloomington, Indiana) enables control of the tip and substrate potentials. In addition to the basic SECM, a lock-in amplifier (SR850, Standford Research Systems, Sunnyvale, California) was used to provide the high frequency ac bias and to demodulate the ac response (high frequency current). A piezo electric "pusher" (PZL-30, Burleigh Instruments, Fishers, NY) with a sensitivity of

0.2 μm/V and a high-voltage amplifier (PZ-150M, Burleigh) was used for fine distance control.

Results and Discussion

Impedance Mode Controller Figure 1 is a schematic overview of the impedance mode controller. The internal generator (FG) of the lock-in amplifier, LIA, is used to produce a small sinusoidal ac bias voltage of 10 mV rms (28 mV p-p) at a frequency between 50 and 90 kHz. The ac bias is applied to external bias voltage input (E_W in) of the potentiostat, which generates an ac bias between the tip and auxiliary electrode. A resistor-capacitor network is used to separate the tip current into a low-frequency component containing the electrochemical information and a high frequency component containing the impedance information. The series combination of a 1 kΩ resistor, R_m, and 10 nF capacitor provides a low impedance path to ground for the ac signal but blocks the low frequency "dc" signal. A 100 kΩ resistor, R_t, at the preamplifier input produces a high-impedance path for the ac signal (compared to the R_mC path). Note that 100 kΩ produces negligible iR drop at the current levels used in these experiments. The voltage drop across R_m is demodulated by the LIA to produce a voltage proportional to the reciprocal of the tip impedance (i.e. the admittance). After amplification, the LIA output is connected to a home-built feedback controller. An output time constant of 0.1 to 30 ms was used on the LIA.

The controller is similar to analog controllers used in STM operation[32, 33] and also has been used for constant-distance imaging by TPM.[13] A complete schematic is available from the authors upon request. Differential amplifier D subtracts the set point reference from the LIA output. The resultant error signal is amplified and integrated at

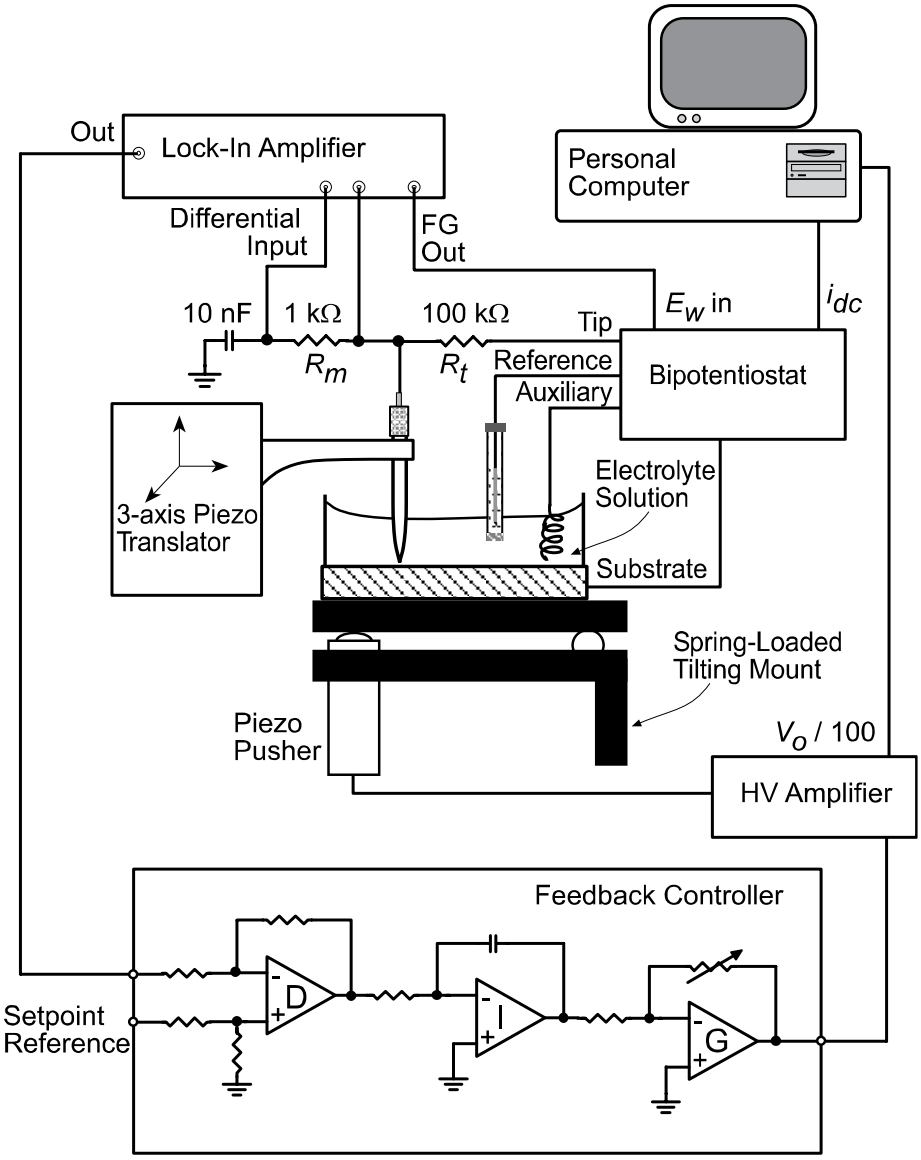

Figure 1. Schematic diagram of the SECM with the impedance feedback controller.

amplifier I (0.8 ms time constant). After integration, the output is amplified further (if necessary) and sent to a HV amplifier. In general, the amount of gain required adjustment for each experiment. The HV output of the amplifier was biased to about the midpoint of its rated output (0–100V) to allow for positive and negative movements

of the piezo driver. The pusher was mounted on a miniature adjustable angle mount (L37-922, Edmonds Industrial Optics), which moves the substrate as required and provides a mechanical amplification of the pusher movement. The piezo movement is proportional to the output of the HV amplifier, which provided relative topographic information about the surface. Because the distance between the tip and pivot point of the lever mount changed from experiment to experiment, the displacement was calibrated for each experiment. Calibration was accomplished by using the inchworm motors to move a fixed distance (typically 10 μm) while the feedback controller was active and noting the corresponding restoring change in output of the HV amplifier. Typically, the sensitivity was found to be about 0.3 μm/V.

Impedance Measurements The resistance to current flow between an embedded disk electrode and a remote counter electrode is concentrated in the solution near the disk surface.[34] In fact, a strong parallel exists between the change in tip conductance and tip current as the tip approaches a substrate. In either case, the presence of a blocking barrier prevents mass transport of electroactive (negative feedback) or ionic (conductivity) species to the tip. Bard and coworkers demonstrated this relationship by equation 1.[27]

$$R_{sol,\infty}/R_{sol}(L) = i_T(L)/i_{T,\infty} \quad (1)$$

Where $R_{sol,\infty}$ and $i_{T,\infty}$ are the resistance and faradaic current, respectively, of the tip electrode in the absence of a blocking surface and $R_{sol}(L)$ and $i_T(L)$ are the resistance and faradaic current at a blocking surface as a function of L (where L is d/a, d = tip-substrate distance, a = electrode radius). Equation 2 is an approximation to the tip current for negative feedback at an embedded disk electrode with RG = 10 (RG is the ratio of insulator to electrode diameter).[35]

$$\frac{i_T(L)}{i_{T,\infty}} = \frac{1}{0.292 + 1.515/L + 0.6553\exp(-2.4035/L)} \quad (2)$$

Given the above relationship between tip current and distance, the change in resistance can provide the tip-substrate separation. This method has been used to initially position ion-selective electrodes by noting the change in tip resistance with distance during a tip approach.[27-29]

These results suggested that a continuous impedance measurement would provide distance information that could then be applied to the problem of constant-distance imaging. A constraint is that the impedance measurement must not interfere with the normal electrochemical measurement. We therefore apply a high-frequency ac voltage bias to the electrochemical cell, which permits the low-frequency faradaic information to be isolated from the high-frequency impedance measurement. Demodulation of the ac tip current provides information about the magnitude, R, and phase, Θ, and of the current passing between the auxiliary and tip electrode. However, the impedance at a UME tip is dominated by the double-layer capacitance even at very high frequencies. For a simple model of the tip impedance as the series combination of the solution resistance, R_{sol}, and double-layer capacitance, C_d, the change in impedance with tip-substrate separation can be calculated. The magnitude of the impedance, Z, is given by

$$Z = \sqrt{[R_{sol}(L)]^2 + X_c^2} \quad (3)$$

where X_c is the capacitive reactance and is given by

$$X_c = \frac{1}{2\pi f C_d} \quad (4)$$

C_d is assumed to be independent of d and frequency, f. Figure 2 is an example calculation for a 10 μm diameter electrode with C_d = 16 pF and $R_{sol,\infty}$ = 5 kΩ at frequencies of 10, 100, and 1000 kHz. The results are plotted semi logarithmically due to the large range in Z values. It is clear that frequencies in the MHz range are necessary before the solution resistance dominates the impedance at the tip (compare to R_{sol} (L) on the plot). However, since the LIA is limited to frequencies less than 100 kHz, the impedance measurement is dominated by the capacitance in this work. Despite the large background, the inset illustrates that there is a measurable change in impedance at small d values. An advantage of the LIA is that it can produce quadrature

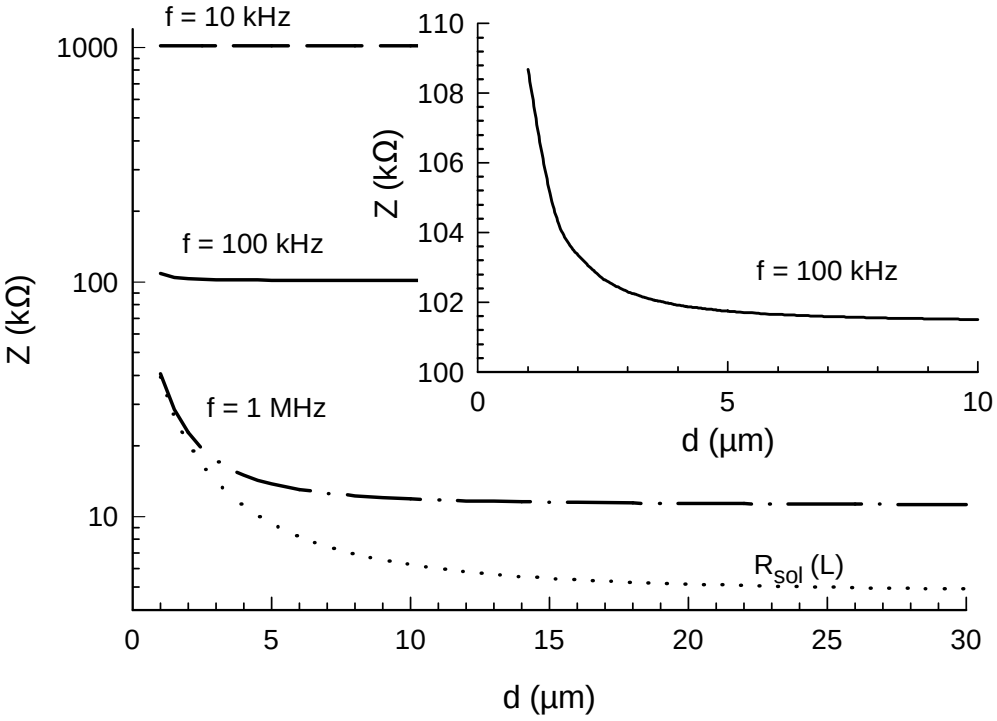

Figure 2. Plot of the impedance magnitude versus tip-substrate separation at frequencies of (– · –) 1 MHz, (——) 100 kHz, and (– – –) 10 kHz. (···) Plot of R_{sol}(L) versus distance. All calculations assumed conditions appropriate for a 10 μm diameter Pt disk electrode (RG = 10), $R_{sol,\infty}$ = 5 kΩ, and C_d = 16 pF. (Inset) detailed view of the 100 kHz response.

outputs (i.e. X and Y), which give the relative contributions of real and reactive components of the impedance signal. Thus, monitoring the X output should provide information about only the resistive component of the impedance and thereby eliminating the offset produced by the capacitive component. However, our preliminary experiments suggested that the X signal component was noisier than the R (magnitude) signal and so R was used in preference to X for all the results shown here.

The R value detected by the LIA is the rms value of the voltage difference across the 1 kΩ measuring resistor on the filter. Figure 3 shows the change in R for a frequency scan from 8 to 100 kHz measured at a 10 μm electrode in a 2 mM $Ru(NH_3)_6Cl_3$ / pH 3.2 buffer. The graph shows the general shape expected for this size electrode. R increases at higher frequencies due to the lower impedance of the capacitance and the curvature arises from the presence of the constant solution resistance. Although higher frequencies produce the largest signals, they often show higher noise levels. For each experiment, a plot of R vs. F was used to choose a frequency that gave a good signal level but low noise. At a given frequency, the impedance measurement is very stable when the tip is far away from the surface, but as the scanning electrode approaches the surface, the tip resistance increases, decreasing R. Figure 4 shows a typical result for the R change as the tip approaches an insulating (A) and conducting (B) substrate. In either case, the R value decreases, which illustrates the key point that the ac current is blocked by both an insulating or conducting surface. In addition, the R values do not decrease to zero, which is expected given the capacitive component. Figure 4 also shows the dc feedback current response of the tips. During the impedance measurements, the electrode was biased to –300 mV vs. Ag/AgCl, which puts it on the plateau of the steady-state wave of the $Ru(NH_3)_6^{3+}$ ion. The dc electrochemical current

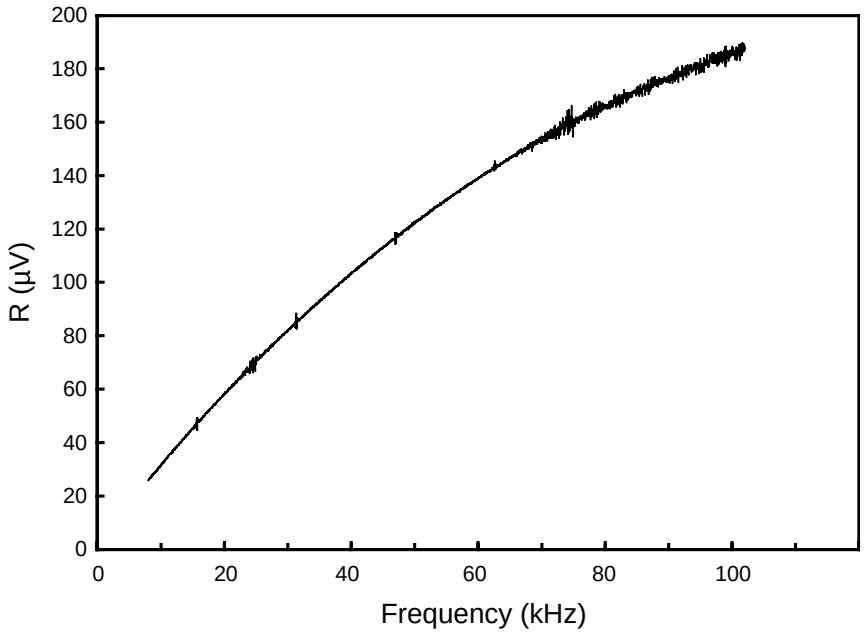

Figure 3. LIA magnitude, R, output for a frequency scan from 8 to 100 kHz at a 10 μm diameter Pt disk electrode in a 2 mM $Ru(NH_3)_6Cl_3$ / pH 3.2 solution Ac bias = 10 mV rms.

was recorded simultaneously with the impedance measurement and shows the expected negative (A) and positive (B) feedback approach curves to the insulating and conducting substrates, respectively. It should be noted that the absolute values for R on the lock-in amplifier are not the same in Figure 4A and 4B because they were acquired during separate experiments. However, the impedance signal always shows the same general response for all of the experiments we have conducted: a decrease in signal when the tip is within one electrode diameter of the surface. Thus, the R value provides a separate signal that allows control of the tip-sample separation independently of the electrochemical reactions occurring at the tip or the substrate. However, it should be noted that the magnitude of R sometimes changes when the dc offset is changed at the tip electrode. The reasons for this are unclear and are under

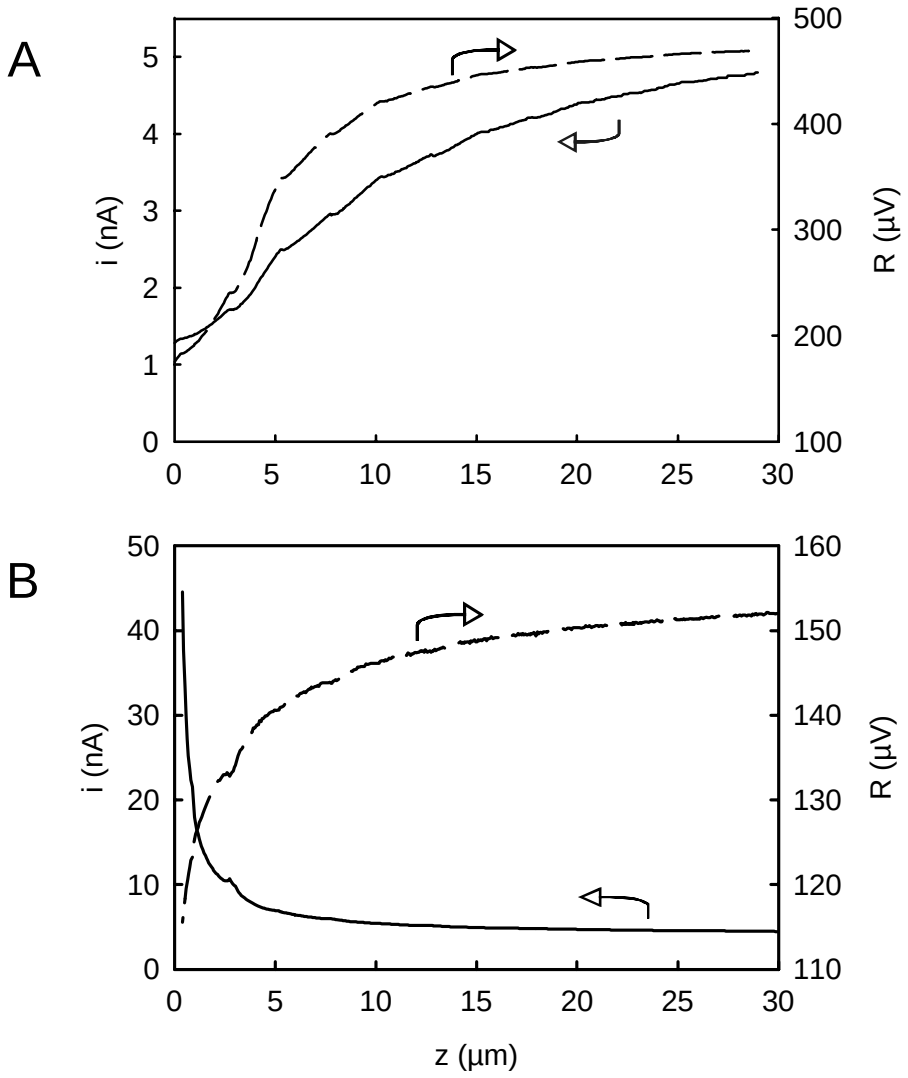

Figure 4. Approach curves of a 10 μm diameter Pt disk electrode to a (A) insulating Teflon or (B) conducting Pt surface in a 2 mM $Ru(NH_3)_6Cl_3$ / pH 3.2 solution for simultaneous electrochemical and impedance measurements. (——) electrochemical feedback response for the tip held at –300 mV vs. Ag/AgCl reference. (– – –) R output for a 10 mV rams ac bias at 73 kHz.

investigation. We feel that the cause is likely due to adsorption/desorption or oxidation reactions at the electrode surface. In any event, this did not prevent use of the R value in the feedback controller.

Little effect of the ac bias is noted in the dc electrochemical response of Figure 4. Further evidence is given in Figure 5, which shows a cyclic voltammogram (CV) acquired at a 10 μm Pt disk electrode in 2 mM $K_3Fe(CN)_6$ / 0.5 M KCl while an ac bias of 10 mV rms and 73.5 kHz was applied to the external input of the bipotentiostat. The potential axis shows the effect of the ac bias (note that the ac is aliased by the lower data collection frequency) since the recorded potential axis is the summation of the CV voltage sweep and the added ac bias. The current does not show oscillations, which indicates that the low and high frequency components are effectively separated.

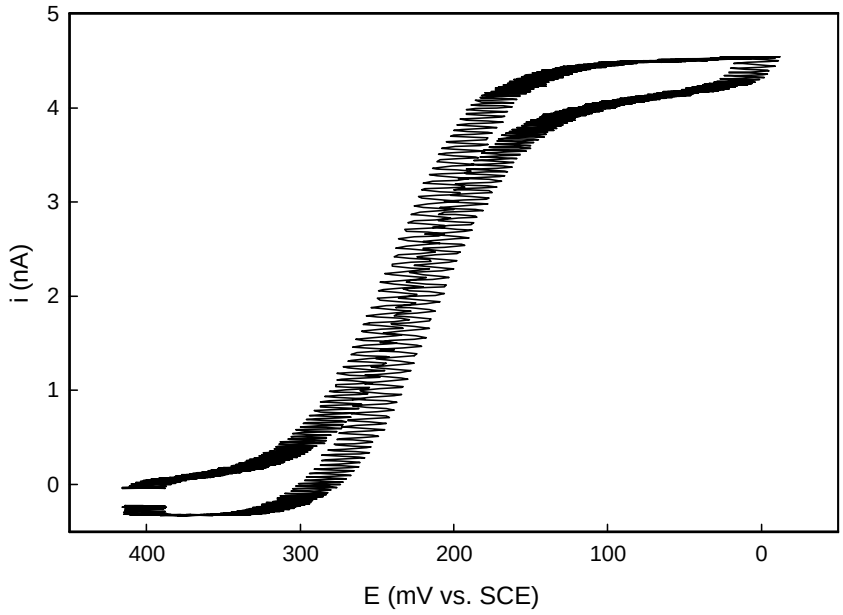

Figure 5. Cyclic voltammogram of 2 mM $K_3Fe(CN)_6$ in 0.5 M KCl / pH 2.0 solution at a 10 μm diameter Pt disk electrode at a scan rate of 100 mV/s. Data collected while applying a 10 mV rms, 73.5 kHz sinusoidal ac bias to the electrode potential.

Impedance Mode Imaging Prior to imaging with the impedance mode an appropriate R set point value is selected from a tip approach curve obtained with the feedback controller turned off. The tip is then withdrawn from the surface using the

coarse z positioners. The feedback controller is turned on, causing the pusher to fully extend. The tip is then moved toward the surface with the coarse z positioners until the R value matches the set point value, at which point the piezo pusher retracts to maintain R at the set point. Once the controller is "in feedback", the controller gain is adjusted to avoid oscillations during imaging. The image in Figure 6A is a feedback mode image acquired with the impedance controller turned on. Note that "feedback mode" is used in SECM to refer to a particular type of SECM image in which an added mediator is used to produce either "negative" or "positive" feedback at insulating or conducting surfaces. A feedback mode image does not require a feedback-based servo controller to make an image. The two uses of the word feedback are separate and, unfortunately, sometimes confused. The image is of a 10-μm diameter Pt electrode sealed in a glass capillary and embedded in epoxy resin. The probe electrode is a 10 μm electrode Pt disk and the solution is 2 mM $K_3Fe(CN)_6$, 0.5 M KCl, pH 2.0. High current on the graph corresponds to the conducting Pt surface, and the lower perimeter currents correspond to the insulating glass around Pt wire. The corresponding topographic image, Figure 6B, indicates a tilted surface with a 6 μm difference in height from where the electrode started the collection of data to the point where the scan ended. Actually, the topographic image indicates that the piezo pusher was at full extension near the end of the scan, which is indicated by a slight leveling of the slope at the back corner of the image. The feedback image indicates the result one would expect for a perfectly flat substrate, i.e. the conducting region is uniformly higher in current than the surrounding insulator and the current in the surrounding insulator is all at the same level (except as noted in the rear of the image where control is lost). There are no other topographic features apparent in the image. The resolution is insufficient with the

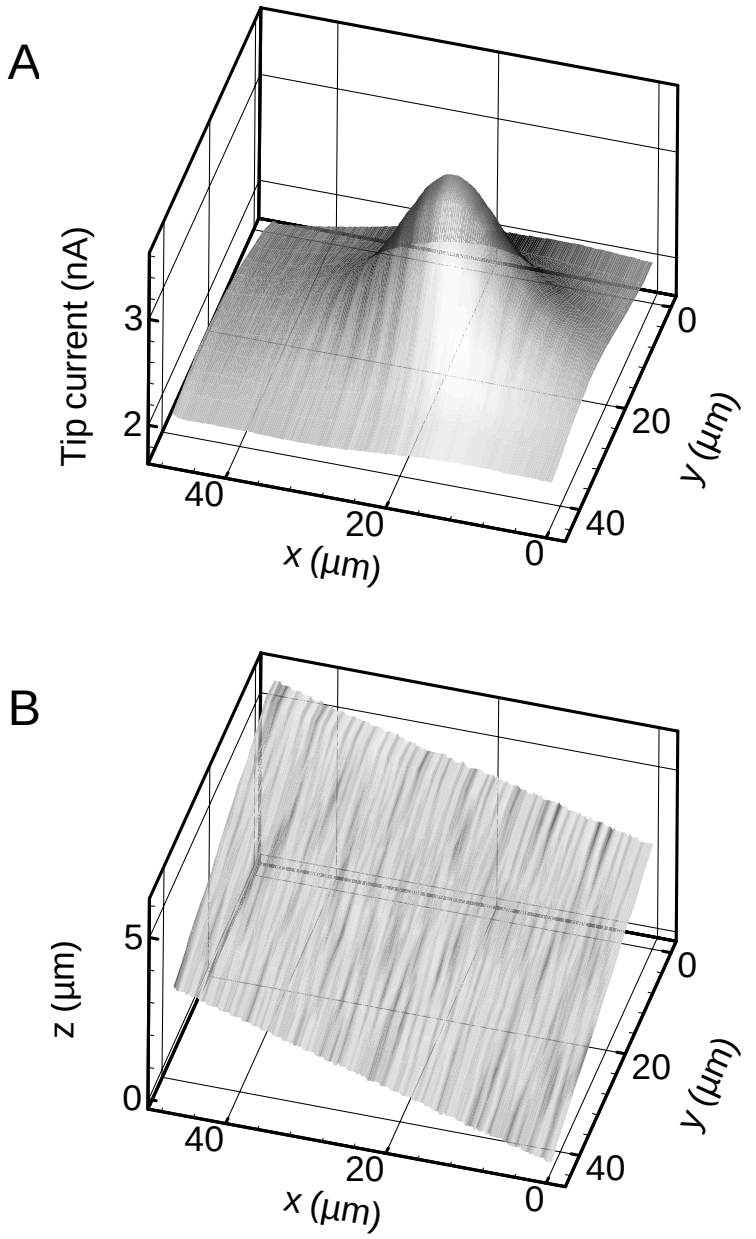

Figure 6. Feedback (A) and topographic (B) height images of a 10 μm diameter Pt disk substrate acquired under impedance feedback control. The topographic images show relative upward movement of the tip. Image data were acquired using a 10 μm diameter Pt tip at 150 mV vs SCE in 2 mM $K_3Fe(CN)_6$, 0.5 M KCl, pH 2.0 solution. The substrate potential was 400 mV and $i_{T,\infty}$ = 3.5 nA. Tip scan rate was 10 μm/s at a separation of about 3 μm with a 10 mV rms ac bias at 90 kHz.

10 μm diameter tip to resolve smaller features. One interesting aspect to the figure is that the positive feedback current is not as large as predicted by theory. Since, the tip and substrate are the same size, the highest current is expected when the tip and substrate are coaxially aligned over each other.[36] In this scan, the resolution is only 4 μm along the x direction, which allows the tip and substrate to miss a coaxial alignment by up to 2 μm.

Impedance mode control was also tested in the GC mode by generating $Fe(CN)_6^{4-}$ at various potentials at the 10 μm substrate electrode. The tip was set to an oxidizing potential to detect $Fe(CN)_6^{4-}$ during imaging. In this experiment, the GC mode is only approximated since some feedback will occur, especially at more negative substrate potentials. GC and topographic images are shown in Figure 7, corresponding to different potentials on the substrate electrode. Performance was satisfactory at all the different potentials and the controller was able to follow the contour of the sample. As expected, the GC images change in appearance at different substrate potentials due to the higher $Fe(CN)_6^{4-}$ concentration at more negative substrate potentials. The location of the substrate is clearly observed by the circular region of higher anodic tip current (drift in the positioners cause the location to shift slightly between images). The topographic images all show about a 4 μm tilt and are similar but not identical in appearance. A concern with the impedance method is that a local change in ionic composition will cause the measured tip impedance to change. Thus, the impedance would be a function of the local ionic composition as well as tip-substrate separation. This would lead to some difficulty in interpreting more complex samples. There is some evidence to support this in Figure 7C. An area of the image near the substrate electrode appears to present some additional topography. An explanation for this apparent

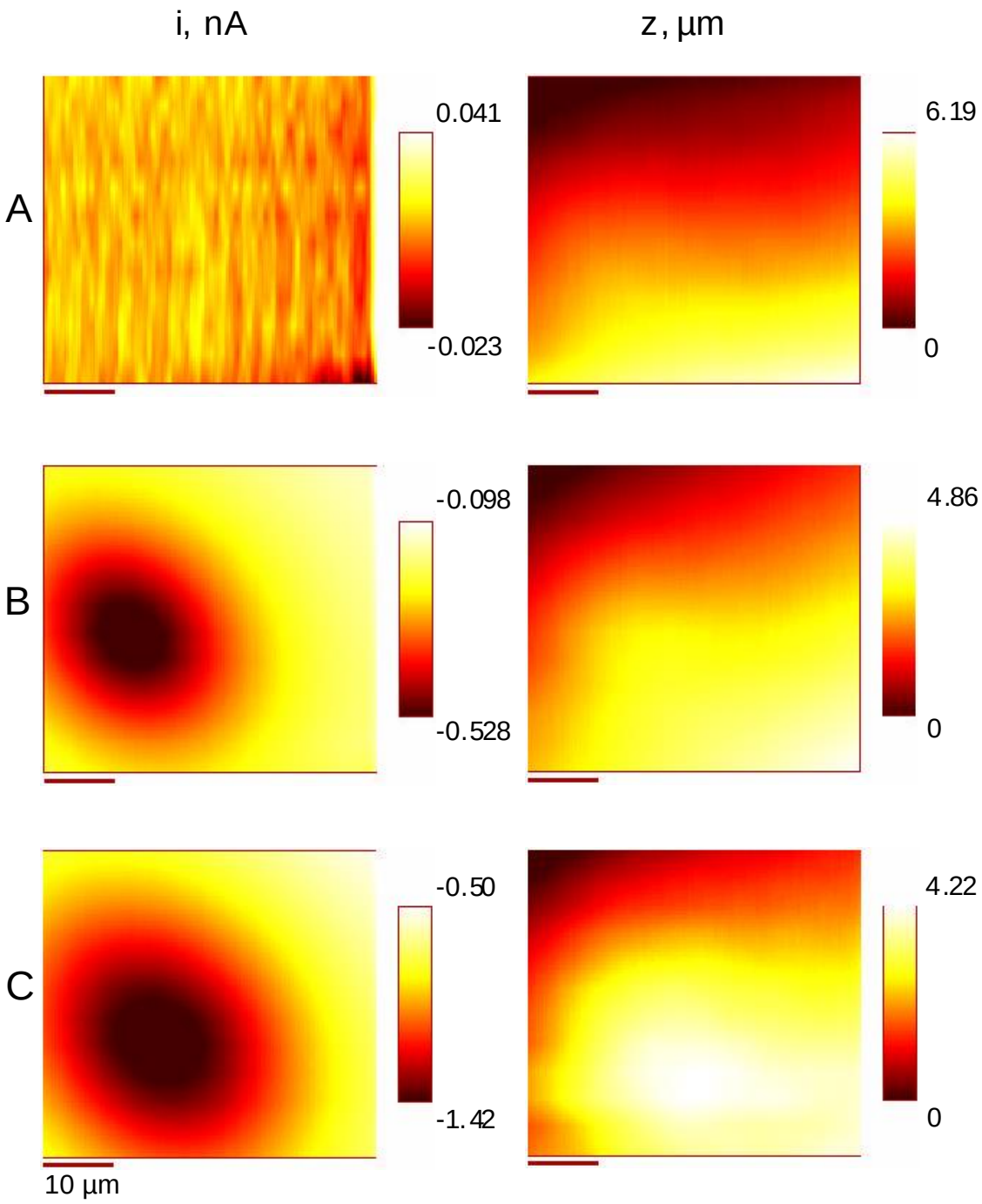

Figure 7. GC (left) and topographic (right) false-color images of a 10 µm diameter Pt disk substrate acquired under impedance feedback control at various substrate potentials. Conditions were similar to Figure 6 except the tip potential was 400 mV vs. SCE and the substrate was (A) 400, (B) 275, and (C) 150 mV vs. SCE.

topography is a change in local conductivity localized at the substrate electrode. This local conductivity is superimposed on the sample tilt, which shifts the apparent maximum of the feature away from the substrate location. This is not observed in Figures 7A and 7B, which are similar except for the local ionic concentration difference. In any event, the effect is subtle and will cause only small changes from the true topography. Another difference between images is the absolute range of the tilt. This is most likely due to drift in the lateral position of the images, which means that the images may have slight changes in topography. Also, if the tip impedance value (i.e. R) drifts with respect to the set point, the topographic data will drift from the true values. Drift in R is a potential problem and can cause loss of feedback control. In these experiments, the R value drifted slightly but not enough to affect an image acquistition. It was found that the R setpoint might need to be adjusted about every hour to maintain the desired tip-substrate separation. Another possibility is that the R value also contains a faradaic component. Further tests need to be conducted to determinate the effect of local solution changes on the conductivity measurement and subsequent effect on observed topography.

The feedback controller was also tested at different R set point values (Figure 8), corresponding to different tip-sample distances. The feedback controller allows the tip to scan closer to the surface as the R set point value was reduced. The only adjustment necessary for closer imaging was to decrease the loop gain of the controller. This is further evidence that the differences in concentrations of the reduced and oxidized species as the electrode gets closer to the polarized substrate do not significantly affect the stability of the voltage drop across the solution between the tip and the substrate.

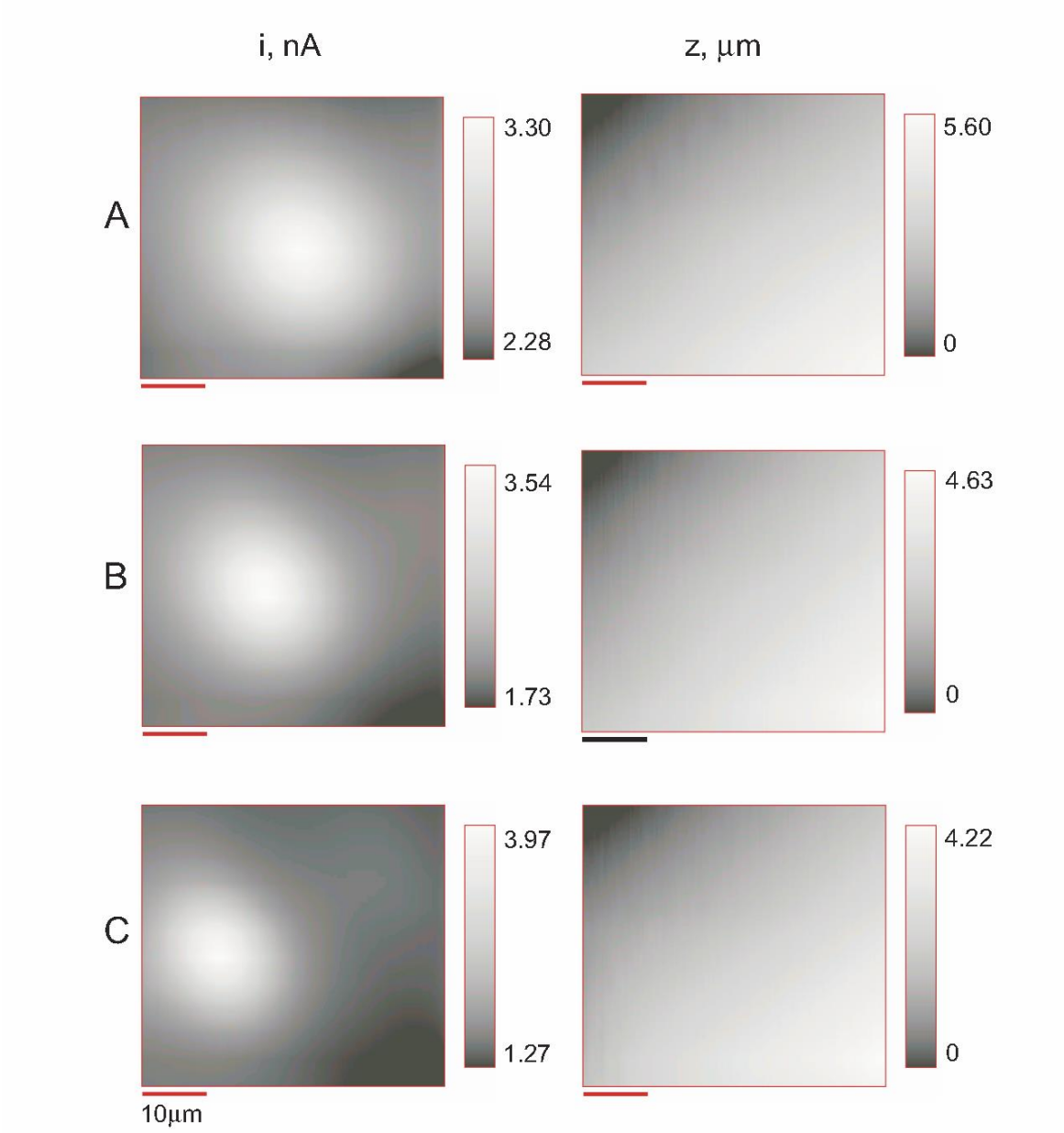

Figure 8. Feedback (left) and topographic (right) grey-scale images of a 10 μm diameter Pt disk substrate acquired under impedance feedback control at different R set point values (i.e. different tip-substrate separations, *d*). Conditions were similar to Figure 6 except the tip potential and substrate potentials were 150 and 400 mV vs. SCE, respectively. (A) R value = 1.95 mV, *d* = 9.4 μm, (B) R value = 1.61 mV, *d* = 6.1 μm and (C) R value = 1.27 mV, *d* = 3.9 μm.

An approach curve obtained with a 2 μm diameter electrode (Figure 9) shows that a tip-sample separation distance of less than 2.0 μm is necessary to see any R value change detected by the LIA. Excellent results were obtained for feedback imaging of the 10 μm diameter substrate electrode at a 2 μm diameter tip (Figure 10). The insulating region of the substrate shows uniformly low current suggesting that topography is eliminated from the feedback image. The conducting region of the image shows some variation in the perimeter and in the center of the electrode. There are also some noise artifacts apparent in the feedback image along the direction of scanning. Comparing the feedback current to theoretical values[35] suggest that the tip was within 1.5 μm of the surface during imaging. The topographic image shows that the

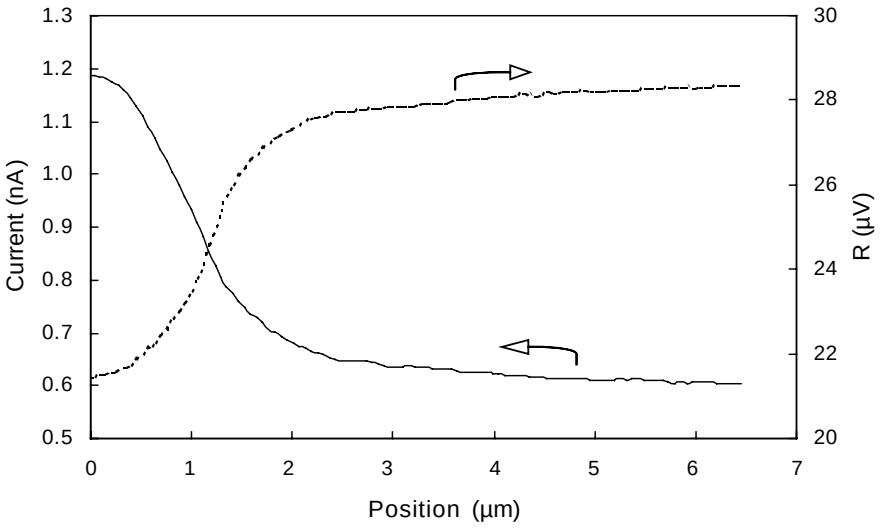

Figure 9. Feedback (A) and topographic (B) height images of a 10 μm diameter Pt disk substrate acquired under impedance feedback control. The topographic images indicate relative upward movement of the tip. Image data were acquired using a 2 μm diameter Pt tip at -320 mV vs Ag/AgCl in 2 mM $Ru(NH_3)_6Cl_3$, pH 3.2 buffer. The substrate potential was 0 mV and $i_{T,\infty}$ = 0.49 nA. Tip scan rate was 1 μm/s at a separation of about 3 μm with a 10 mV rms ac bias at 74 kHz

surface of the substrate had a tilt and also that the conducting region was slightly recessed with respect to the surrounding insulator. This recess explains the depression in the center of the conductor in the feedback image. As the tip moved over the recessed region, the feedback controller moved the tip towards the surface, thus blocking diffusion into or out of the tip–substrate gap. As a result, the feedback current is reduced slightly. Note that this would also tend to increase the tip impedance producing a tendency to retract the tip. On balance, a net movement into the recess occurs. A tip crash is unlikely under these conditions (where a tip enters a recess) since the impedance would increase significantly as the tip approached a collision with the surface.

The impedance mode becomes increasingly challenging at smaller tips. The resistance of a UME is inversely proportional to the electrode radius[37] but the electrode capacitance is proportional to the area. Thus, the increase in background with respect to the signal is proportional to the electrode radius at low frequencies (i.e. where the capacitive reactance is much larger than the resistance). Increasing the ac bias frequency will potentially reduce the background but the LIA has a maximum frequency of 100 kHz. The poorer measurement conditions made it necessary to increase the time constant in the lock-in amplifier to 30 ms (compared to 0.3 ms at the 10 μm electrode) in order to stabilize the impedance measurement sufficiently to allow the feedback controller to work. This high time constant forced us to use slower scan rates (1 μm/s) to be able to collect this data. However it can be seen from the approach curve that once these precautions were taken, the R signal was smooth and stable enough to allow the imaging of the substrate. We believe that replacing the RC filter

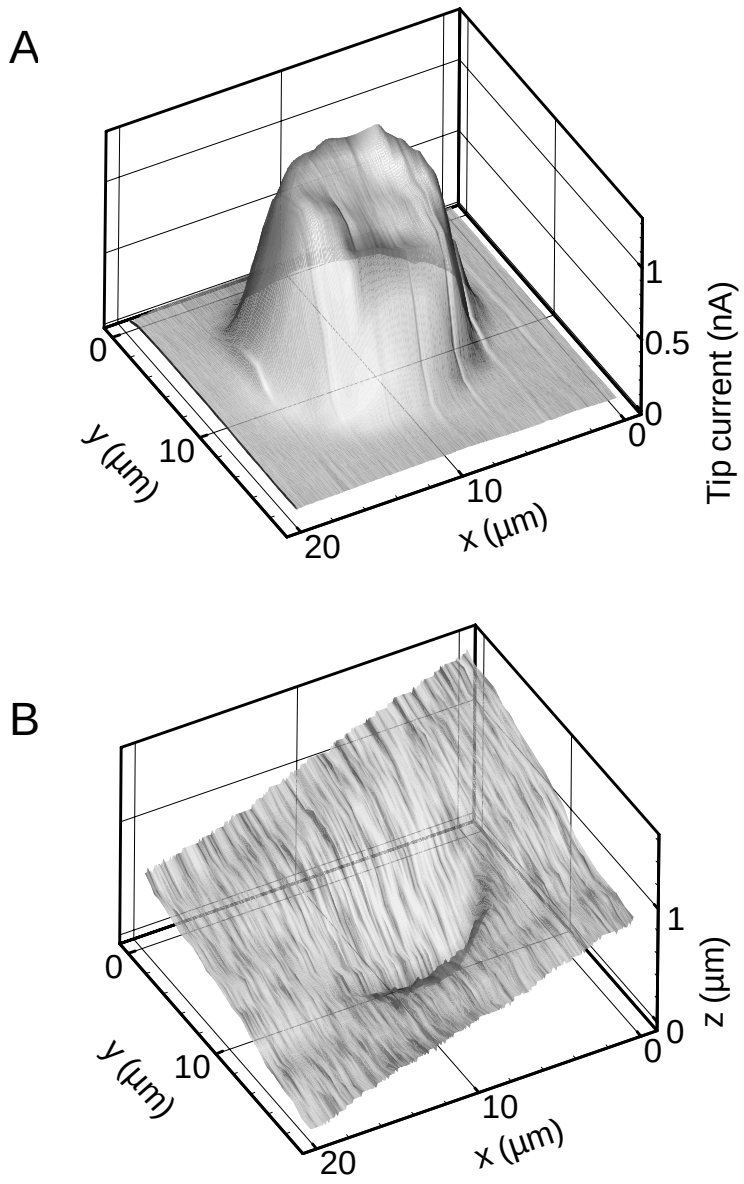

Figure 10. Feedback (A) and topographic (B) height images of a 10 μm diameter Pt disk substrate acquired under impedance feedback control. The topographic images indicate relative upward movement of the tip. Image data were acquired using a 2 μm diameter Pt tip at –320 mV vs Ag/AgCl in 2 mM $Ru(NH_3)_6Cl_3$, pH 3.2 buffer. The substrate potential was 0 mV and $i_{T,\infty}$ = 0.49 nA. Tip scan rate was 1 μm/s at a separation of about 3 μm with a 10 mV rms ac bias at 74 kHz

that we are currently using with a better filter will reduce the noise on both the low and high frequency signals.

Conclusions

We have developed a constant-distance method for SECM based on controlling the tip impedance near the surface of the sample. The method provides independent topographic information as well as electrochemical information on samples containing both conducting and insulating regions and can be used with durable glass-sealed electrodes, eliminating the need for specially built and fragile tips. The method works with positive and negative feedback and the GC mode. The effect of different ionic strengths on imaging has been examined with favorable results.

Future work will focus on optimizing the imaging conditions to increase S/N (and thus increase scanning speed), minimize drift, and allow use at smaller tip electrodes. A focus of these optimizations will be increased attention to the isolation RC circuit and the use of higher measurement frequencies. We are also interested in the possible interference in the impedance measurement by faradaic electrochemistry. It may be possible to measure harmonics of the ac current to compensate for these faradaic processes. Finally, we are aware that the impedance method described here may not work well for non disk-shaped tips. In comparison to the SECM feedback behavior at conical or hemispherical tips,[35] we expect that there will be less change in resistance as the tip approaches a surface. Whether this lower sensitivity will prevent operation of the feedback controller is yet to be determined.

Acknowledgements

The authors would like to acknowledge the National Science Foundation, the State of Mississippi, and the Mississippi EPSCoR program for support by grants DBI-9987028 and EPS-9874669.

References

(1) Bard, A. J.; Fan, F.-R.; Mirkin, M. V. In *Electroanalytical Chemistry*; Bard, A. J., Ed.; Marcel Dekker: New York, 1994; Vol. 18, pp 244-370.

(2) Bard, A. J.; Mirkin, M. V. Eds.; *Scanning Electrochemical Microscopy*, Marcel Dekker: New York, 2001.

(3) Bard, A. J.; Fan, F.-R. F.; Pierce, D. T.; Unwin, P. R.; Wipf, D. O.; Zhou, F. M. *Science* **1991,** *254*, 68-74.

(4) Kwak, J.; Bard, A. J. *Anal. Chem.* **1989,** *61*, 1221-1227.

(5) Basame, S. B.; White, H. S. *Anal. Chem.* **1999,** *71*, 3166-3170.

(6) Wipf, D. O. *Colloid Surf. A* **1994,** *93*, 251-261.

(7) Macpherson, J. V.; Unwin, P. R. *J. Phys. Chem.* **1995,** *99*, 3338-3351.

(8) Tsionsky, M.; Cardon, Z. G.; Bard, A. J.; Jackson, R. B. *Plant Physiol.* **1997,** *113*, 895-901.

(9) Lee, C. M.; Kwak, J. Y.; Bard, A. J. *Proc. Natl. Acad. Sci. USA* **1990,** *87*, 1740-1743.

(10) Scott, E. R.; Phipps, J. B.; White, H. S. *J. Invest. Dermatol.* **1995,** *104*, 142-145.

(11) Macpherson, J. V.; Beeston, M. A.; Unwin, P. R.; Hughes, N. P.; Littlewood, D. *Langmuir* **1995,** *11*, 3959-3963.

(12) Yasukawa, T.; Kaya, T.; Matsue, T. *Chem. Lett.* **1999**, 975-976.

(13) Wipf, D. O.; Bard, A. J.; Tallman, D. E. *Anal. Chem.* **1993,** *65*, 1373-1377.

(14) Wipf, D. O.; Bard, A. J. *Anal. Chem.* **1992,** *64*, 1362-1367.

(15) Barenz, J.; Hollricher, O.; Marti, O. *Rev. Sci. Instrum.* **1996,** *67*, 1912-1916.

(16) Karraï, K.; Grober, R. D. *Ultramicroscopy* **1995,** *61*, 197-205.

(17) Ludwig, M.; Kranz, C.; Schuhmann, W.; Gaub, H. E. *Rev. Sci. Instr.* **1995,** *66*, 2857-2860.

(18) Garfias-Mesias, L. F.; Smyrl, W. H. *J. Electrochem. Soc.* **1999,** *146*, 2495-2501.

(19) Buchler, M.; Kelley, S. C.; Smyrl, W. H. *Electrochem. Solid-State Lett.* **2000,** *3*, 35-38.

(20) Garfias-Mesias, L. F.; Smyrl, W. H. *Electrochim. Acta* **1999,** *44*, 3651-3657.

(21) Hengstenberg, A.; Blöchl, A.; Dietzel, I. D.; Schuhmann, W. *Angew. Chem. Int. Ed.* **2001,** *40*, 905-908.

(22) Zu, Y.; Ding, Z.; Zhou, J.; Lee, Y.; Bard, A. J. *Anal. Chem.* **2001,** *73*, 2153-2156.

(23) Macpherson, J. V.; Unwin, P. R. *Anal. Chem.* **2001,** *73*, 550-557.

(24) Hansma, P. K.; Drake, B.; Marti, O.; Gould, S. A. C.; Prater, C. B. *Science* **1989,** *243*, 641-643.

(25) Zhang, H. J.; Wu, L.; Huang, F. *J Vac Sci Technol B* **1999,** *17*, 269-272.

(26) Korchev, Y. E.; Gorelik, J.; Lab, M. J.; Sviderskaya, E. V.; Johnston, C. L.; Coombes, C. R.; Vodyanoy, I.; Edwards, C. R. W. *Biophys J* **2000,** *78*, 451-457.

(27) Horrocks, B. R.; Schmidtke, D.; Heller, A.; Bard, A. J. *Anal. Chem.* **1993,** *65*, 3605-3614.

(28) Wei, C.; Bard, A. J.; Nagy, G.; Toth, K. *Anal. Chem.* **1995,** *67*, 1346-1356.

(29) Kashyap, R.; Gratzl, K. *Anal. Chem.* **1999,** *71*, 2814-2820.

(30) Wightman, R. M.; Wipf, D. O. In *Electroanalytical Chemistry*; Bard, A. J., Ed.; Marcel Dekker: New York, 1989; Vol. 15, pp 267-353.

(31) Wipf, D. O.; Bard, A. J. *J. Electrochem. Soc.* **1991,** *138*, 469-474.

(32) Pohl, D. W. *IBM J. Res. Develop.* **1986,** *30*, 417-427.

(33) Park, S.-I.; Quate, C. F. *Rev. Sci. Instrum.* **1987,** *58*, 2004-2009.

(34) Newman, J. *J. Electrochem. Soc.* **1966,** *113*, 501-502.

(35) Mirkin, M. V.; Fan, F. R. F.; Bard, A. J. *J. Electroanal. Chem.* **1992,** *328*, 47-62.

(36) Bard, A. J.; Mirkin, M. V.; Unwin, P. R.; Wipf, D. O. *J. Phys. Chem.* **1992,** *96*, 1861-1868.

(37) Newman, J. *J. Electrochem. Soc.* **1970,** *117*, 198-203.